THE TRAPPING OF A GUN-INJECTED PLASMA BY A TOKAMAK

by

ANTHONY WILLIAM LEONARD

A thesis submitted in partial fulfillment of the requirements for the degree of

DOCTOR OF PHILOSOPHY

(Physics)

at the

UNIVERSITY OF WISCONSIN-MADISON

1986

THE TRAPPING OF A GUN INJECTED PLASMA

BY A TOKAMAK

Anthony William Leonard

Under the supervision of Professor J. C. Sprott

A Marshall gun was used to refuel a tokamak discharge on the Tokapole II device. Gun injection was able to increase the line-averaged density of the discharge by 50%. The density profile became more peaked due to gun injection.

A model is discussed which describes the trapping of a gun injected plasma in a pure octupole field, due to a depolarization current. This model is expanded to include arbitrary toroidal fields added to the poloidal field. A slowing time, τ_s, is derived for the trapping of an injected plasma of density n_b, and temperature, T_e, into poloidal field, B_p and toroidal field, B_t.

Experimental observation of plasma injected into an octupole field fits the derived slowing relation, with an exception in the beam density dependence. An anomalous resistivity at low field

strengths could account for the conflict, though the nature of this resistivity is not understood.

The more tokamak-like case of injection into poloidal and toroidal fields fits the data. Trapping is seen to be most strongly controlled by the poloidal to toroidal field ratio, B_p/B_t. The slowing time is also inversely proportional to the beam density, n_b.

The experiment is extended to the tokamak discharge by the addition of plasma density and current to the vacuum fields, B_p and B_t. Plasma density is seen to not significantly affect trapping. The increase in trapping with plasma current is explained in terms of additional poloidal field added to the central current channel.

An extrapolation is made of the refueling system to the reactor-size tokamak TFTR. An effective system seems easily obtainable.

ACKNOWLEDGMENTS

I would like to thank my major professor, J. C. Sprott for his continued help in this project. His suggestions and criticisms were invaluable in bringing this work to a conclusion.

I thank professor Richard Dexter for discussions and suggestiors in my research.

Tom Lovell and his technical staff have been of great service when dealing with technical and engineering issues. I wish to thank Jeremy Wight who helped considerably in construction of hardware used for this experiment.

I am grateful to all of my fellow graduate students in plasma physics. They helped with advice and encouragement throughout this work. They were very reasonable in accommodating schedules for use of the experimental devices. I thank all my fellow graduate students not in plasma physics who have provided encouragement and support throughout my stay in Madison.

Finally I wish to most graciously thank my parents, Jack and Irene, who have unfailingly encouraged my education from its beginning.

Financial support has been provided by the United States Department of Energy.

TABLE OF CONTENTS

PLP REPORTS

In this thesis, a number of references are made to the internal reports of the University of Wisconsin Plasma Physics Group. These reports, which are identified by PLP numbers, are available upon request from:

Plasma Physics Office

University of Wisconsin

1150 University Avenue

Madison, Wisconsin 53706

CHAPTER I

INTRODUCTION

As fusion devices have grown larger, plasma refueling has become an issue which has taken on increased significance. This is especially true for the largest machines and those which incorporate divertors. The issue of refueling will have to be investigated and understood before an efficient reactor can be designed and built.

Typically in a plasma device, such as a tokamak, the working gas is puffed in from the outside of the discharge. The gas then penetrates into the discharge before being ionized by the plasma. This provides fuel to the bulk of the plasma. If too much of the gas is ionized near the edge of the discharge, plasma will be trapped by the magnetic field and not reach the hot, central core. In large devices, and those with divertors, there is a large, cool, edge region, which can ionize gas puffed from the outside. In these devices gas puffing would cause the density profile to become very flat. A peaked density profile is much more desirable.

A peaked density profile has several advantages varying from enhanced fusion power production to being important in some schemes of steady state current generation in tokamaks.[1,2] Also the highest energy confinement achieved in tokamaks have a peaked density profile.[3]

A recently developed technique for refueling the center of a tokamak with plasma is the injection of pellets of deuterium ice into the discharge. These fast moving pellets penetrate far into the plasma before being vaporized and ionized. The highest density and energy confinement times in tokamaks have been produced using this method of refueling.[4,5]

An alternative to pellet fueling is gun injection[6]. A Marshall gun, by means of an arc discharge, produces a very dense plasma which travels from the gun at a high rate of speed.[7] If this moving plasma can penetrate into a tokamak discharge and then be stopped in the center, gun injection may provide a new efficient method of refueling a plasma. Marshall guns have the advantage of being a much simpler technology than pellet injectors and could easily be scaled up in size for a reactor. This report details the use of a Marshall gun to refuel the Tokapole II tokamak.

It has been known for some time that a moving plasma can cross magnetic field lines provided the extent of the plasma is smaller than the extent of the field, and it meets the condition[8]

$$1+\omega_{pi}^2/\omega_{ci}^2 \gg 1$$

where ω_{pi} is the plasma frequency of the moving plasma and ω_{ci} is the ion cyclotron frequency in the magnetic field the plasma is crossing.

As a stream of plasma, moving with a velocity $\vec{V}$, encounters a transverse magnetic field, electrons are deflected in one direction and ions in the other direction, due to the Lorentz force. This charge separation builds up an electric field $\vec{E}$ perpendicular to the magnetic field $\vec{B}$. The electric field increases in magnitude until

$$\vec{E} = -\vec{V}\times\vec{B}$$

The bulk of the moving plasma then sees this field and can continue to move with it's original velocity, or

$$\vec{V} = \vec{E}\times\vec{B}/B^2$$

The plasma can do this provided its density is great enough in comparison to the magnetic field strength.

Baker and Hammel showed how a plasma stream moving across magnetic field lines could be stopped if the polarization electric field could be eliminated[9]. An external conductor that connects magnetic field lines of different potential due to the polarization electric field would allow current to flow to short out the electric field. If the inductance of the current path is low enough, the current would build up quickly to stop the plasma in time t if

$$\Delta\rho\vec{V} = -\int_0^t \vec{J}\times\vec{B}dt$$

where ρ is the mass density of a fluid element in the plasma stream and $\vec{J}$ is the current density through that element. The experiments of Baker and Hammel agreed quite well with this model.

Since then plasma guns have been used to fill toroidal octupoles with plasma[10]. These machines have only a poloidal field in contrast to a tokamak which has poloidal and toroidal magnetic fields. For fueling an octupole the moving plasma stream is launched perpendicular to the magnetic field lines. The plasma easily crosses the magnetic field lines until it reaches the center of the machine. Once past the center the plasma encounters field lines in the opposite direction, and thus the polarization electric field switches sign. In this way the magnetic field lines themselves can act as the external conductor to stop the moving plasma.

Finally work by Sprott and Strait showed that an octupole field with an applied toroidal field and with an existing plasma could still trap an injected plasma.[11] This was as close an experiment to refueling a tokamak as has been done using a gun. All of these past encouraging results have led us to test refueling a tokamak with plasma gun injection.

This thesis consists of two parts. The first is concerned with showing the feasibility of using a Marshall gun as a means of refueling a tokamak. Important topics such as an immediate increase in density and peaking of the density profile are documented. Other issues such as confinement time improvement and impurity generation

are also briefly discussed. These are issues that are of concern to the fusion community and need to be addressed when comparing various refueling schemes.

The second part of this thesis deals with understanding the injection process itself. The trapping of injected plasma is seen within the framework of a depolarization current mechanism. The theoretical considerations of this mechanism are explored for the case of plasma injected into a combination of poloidal and toroidal fields. The theoretical model is then compared to the experimental observations of injection into Tokapole II. The previous work in this area is extended by injection into poloidal fields with an added strong toroidal field, and finally the injection of plasma into a tokamak discharge is studied. The experiments are seen to agree reasonably with the mechanism described.

B. Outline of Thesis

Chapter 2 contains a brief description of the experimental apparatus. The properties of Tokapole II along with the Marshall gun are described. Also the experimental diagnostics are briefly explained.

Chapter 3 contains a description of the refueling process. This includes issues relevant to the fusion community such as profile peaking, confinement times and impurity production.

In chapter 4 a theoretical model of the trapping process is derived. This model, based on a depolarization current mechanism, describes the injection of plasma into a combination of poloidal and toroidal fields.

Chapter 5 consists of trapping experiments that were carried out in vacuum fields with no plasma present as an extension of previous work of injection into octupoles. This is a bridge to the tokamak refueling case.

Chapter 6 describes experiments done with trapping of injected plasma in a tokamak discharge. This is compared with the earlier theoretical description. Other possible trapping mechanisms are discussed, with a final discussion of the trapping model and its accuracy and limitations in describing gun refueling of a tokamak. This chapter also contains an extrapolation of the model to a reactor size experiment with the considerations involved in using a gun to refuel a reactor. Suggestions for further work are also made.

Chapter 8 is a final summary of the conclusions reached in this work.

References for Chapter I

[1]J. Kesner and R. W. Conn, Nucl. Fusion 16, 397 (1976)

[2]N. J. Fisch and C. F. F. Karney, Phys. Fluids 24, 27 (1981)

[3]R. J. Fonck, et al., Proceedings of the sixth International Conference on Plasma Surface Interactions in Controlled Fusion Devices, Nagoya, Japan, May 1984 J. Nucl. Mater.(Netherlands) 128, 330 (1984)

[4]ibid.

[5]M. Greenwald, D. Gwinn, S. Milora, J. Parker, R. Parker, S. Wolfe, et al., Phys. Rev. Lett. 53, 352 (1984)

[6]E. Ott and W. M. Manheimer, Nuclear Fusion 17, 1057 (1977)

[7]J. Marshall, Phys. Fluids 3, 134 (1966)

[8]G. Schmidt, Phys. Fluids 3, 961 (1960)

[9]D. A. Baker and J. Hammel, Phys. Fluids 8, 713 (1965)

[10]R. A. Dory, D. W. Kerst, D. M. Meade, W. E. Wilson, and C. W. Erickson, Phys. Fluids 9, 997 (1966)

[11]E. J. Strait and J. C. Sprott, Nuclear Fusion 18, 1595 (1978)

CHAPTER II

APPARATUS AND DIAGNOSTICS

A. Tokapole II

The experiments for this thesis were carried out in Tokapole II,[1] (Figure 2-1), a 4-node poloidal divertor tokamak which has been in operation at the University of Wisconsin-Madison Physics Department since 1978. A complete description of the engineering and physics considerations involved in the design of the device can be found in references 2 and 3.

The vacuum vessel consists of a 44 cm square cross section torus with a major radius of 50 cm (figure 2-2). The vessel wall is constructed of 3-cm-thick aluminum with insulated breaks both toroidally and poloidally to allow magnetic fields to enter. The poloidal divertor configuration is generated by four, high conductivity, chromium-copper-alloy hoops which are electrically insulated from the tank. Each of these 5 cm diameter hoops is supported inside the vessel by three rods made of a high tensile strength beryllium copper alloy. The vertical position of these hoops may be varied by ±5.0 mm and has been adjusted to create an optimal tokamak discharge.

Figure 2-1. Tokapole II.

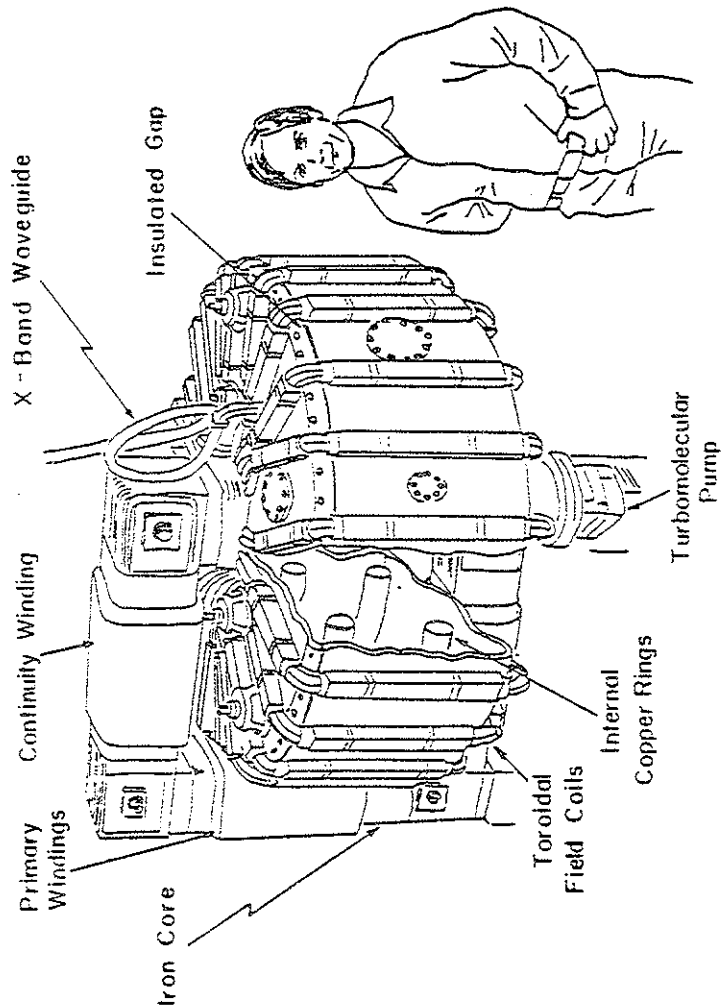

Figure 2-1

Figure 2-2. Cross section of vacuum vessel showing the internal hoops.

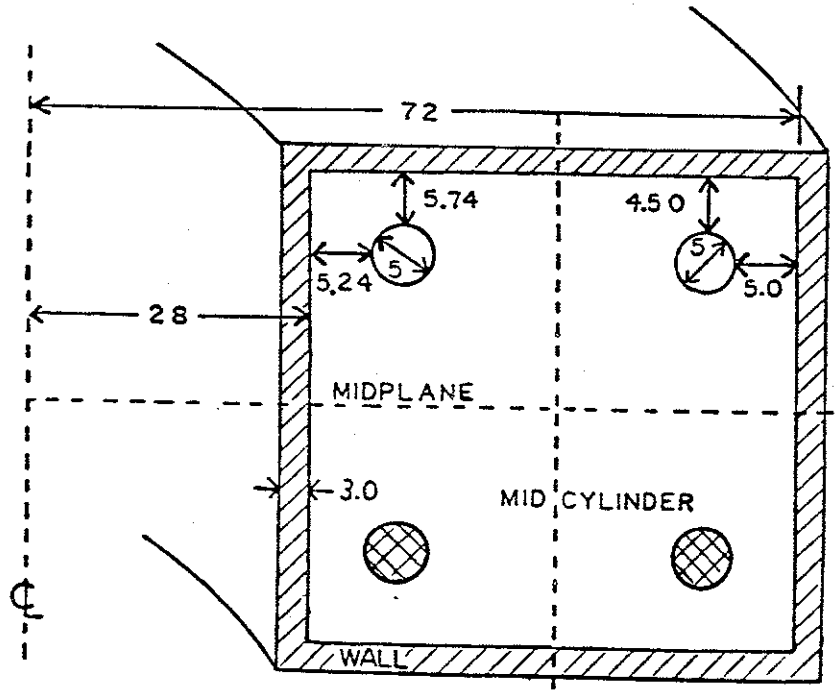

Figure 2-2

Current in the internal hoops and plasma is driven inductively by a 7.2 mF, 5 kV (90 kJ) capacitor bank through an iron core transformer. The 40:1 turns ratio on the transformer gives a sinusoidal field shape in time which has a half period of 5.6 msec. The poloidal field can be crowbarred actively by adding a 450 V, 0.96 F (97 kJ) capacitor bank. A damping resistor can also be added to the circuit to shorten the initial voltage spike. The damped and undamped poloidal circuit voltage waveforms are shown in figure 2-3.

The toroidal field, shown in figure 2-3, is created by external windings driven by a 52 mF, 5 kV (650 kJ) capacitor bank, which is passively crowbarred with a half period of 10 msec. The toroidal field is typically fired 6 msec before the poloidal field, leading to a relatively constant toroidal field for the duration of the discharge. A typical value for the toroidal field on axis for a tokamak discharge is 5 kG.

For these experiments Tokapole II was run in one of two modes. The first was an octupole mode. In this case the poloidal field was created by the inductively driven internal hoops alone, i.e. no plasma current. This was done by applying the undamped voltage waveform to the primary of the transformer, without puffing gas into the vacuum vessel. This configuration, with a total hoop current of 200 kA, produced a flux plot similar to that shown in figure 2-4. This mode was very similar to previous octupole experiments in which gun injection was done. Also an arbitrary toroidal field could be superimposed on to this existing field.

Figure 2-3. The wave form for a) the poloidal gap voltage both damped and undamped. b)the hoop current resulting from the gap voltage, and c) a typical toroidal field waveform.

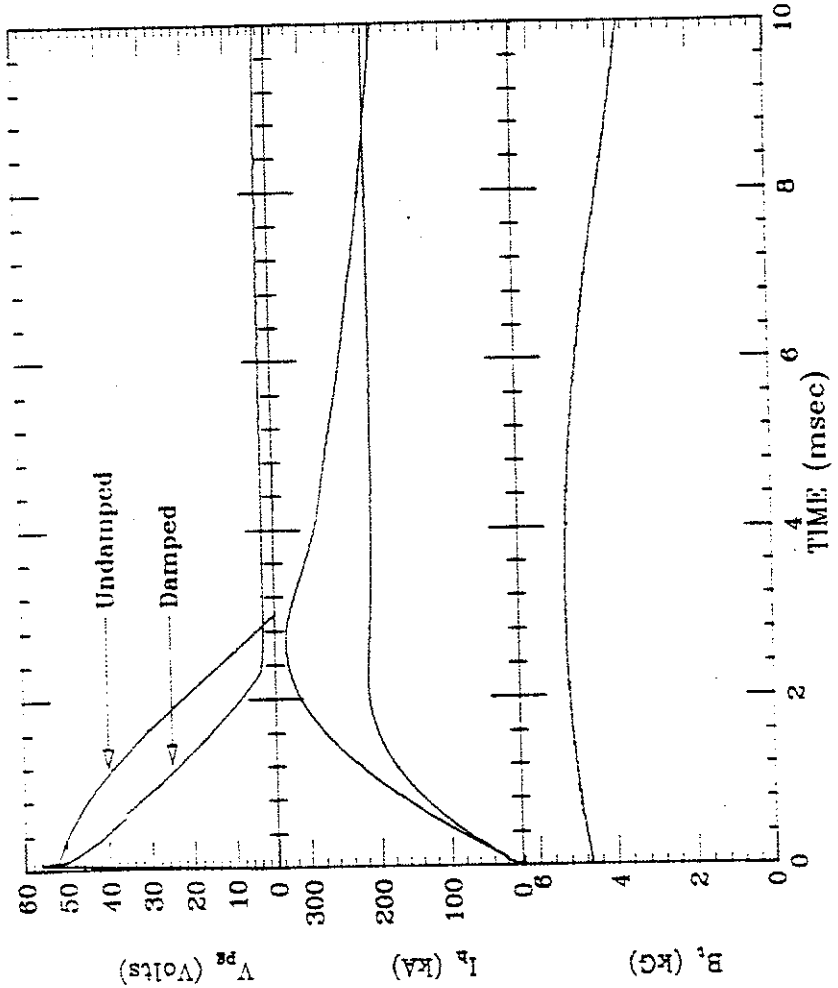

Figure 2-3

Figure 2-4. Vacuum poloidal field flux plot. Contours of poloidal field due to internal hoop current.

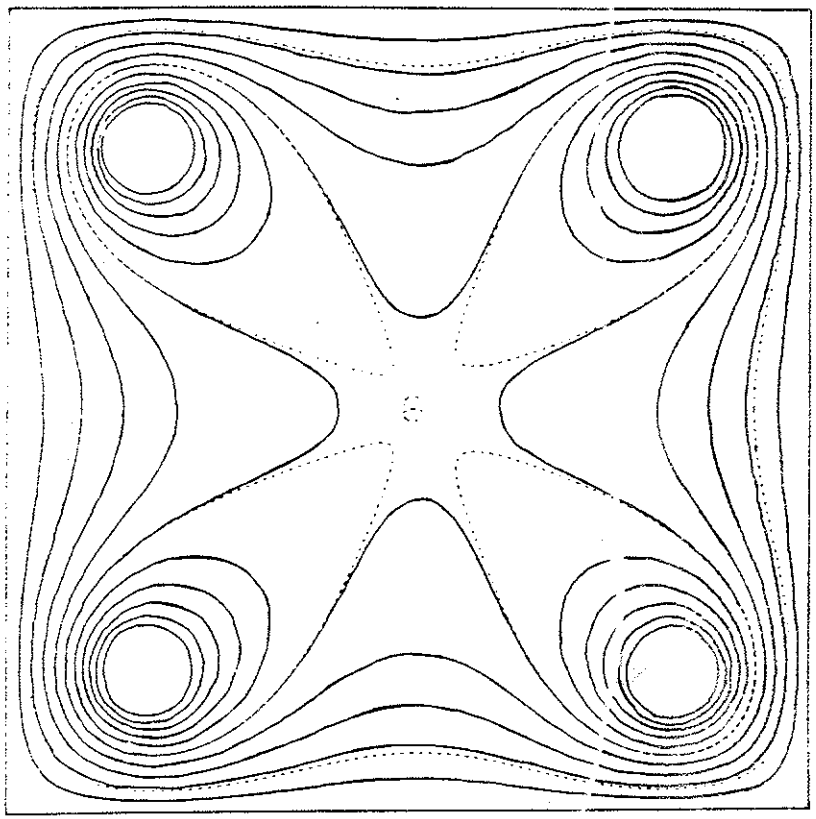

Figure 2-4

The other mode of operation was the divertor tokamak mode. In this case the vacuum vessel was filled to approximately 3×10^{-4} torr with hydrogen by use of a fast piezoelectric puff valve, just prior to the firing of the toroidal field. Microwave preionization (10 kW of 16 GHz) which was resonant with the electron cyclotron frequency of the toroidal field (5 kG) created a weak plasma just before the damped poloidal voltages were fired. A plasma current was then driven down the center of the device in addition to the hoop current. This addition of the plasma current produced a flux plot such as that shown in figure 2-5. This flux plot was calculated with an MHD equilibrium code for parameters that were characteristic of those used in these experiments.

B. Marshall Gun Characteristics

A coaxial Marshall gun was used as the external plasma source for these refueling experiments. The Marshall gun consisted of two concentric barrels, or electrodes. A working gas, hydrogen in this case, was puffed into the region between the barrels. High voltage was then applied between the electrodes, ionizing the hydrogen gas and allowing current to flow between the two barrels. The magnetic field created by this current resulted in a $\vec{J}\times\vec{B}$ force on the plasma which propelled it down the gun barrel, as illustrated in figure 2-6. As the plasma moved down the barrel, the current through it ionized gas as it traveled until ejected from the gun. Typically a

Figure 2-5. Poloidal magnetic flux plot calculated with a MHD equilibrium code for a typical tokamak discharge in Tokapole II.

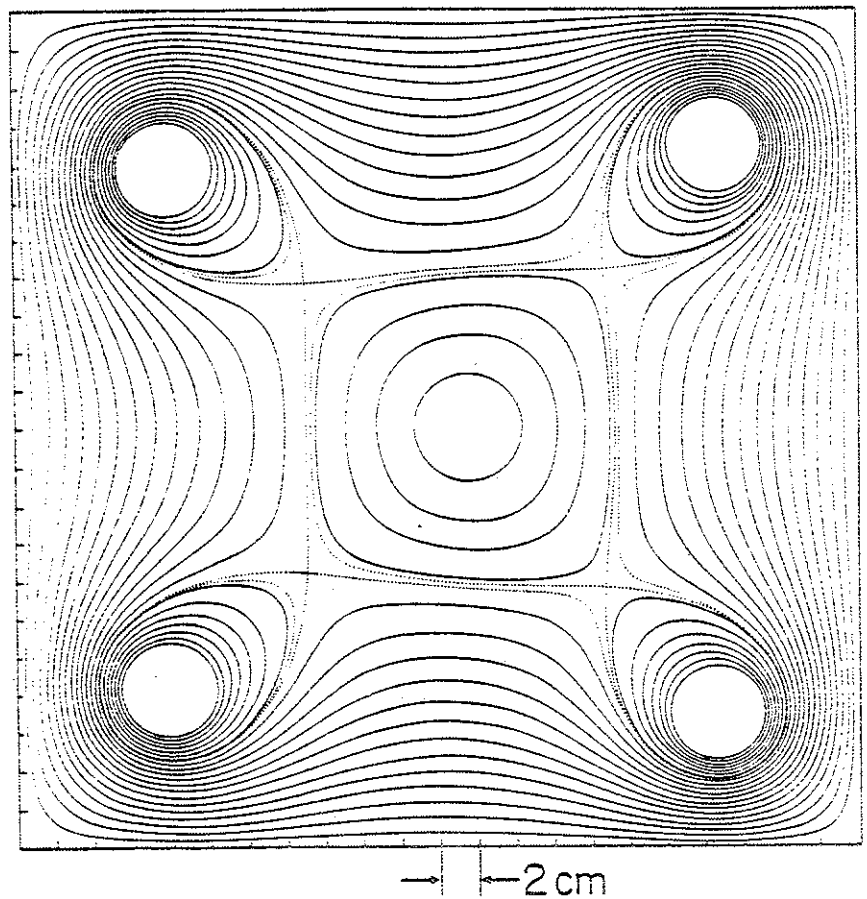

Figure 2-5

Figure 2-6. A Marshall gun discharge is illustrated. High voltage ionizes the gas, and the resultant current creates a $\vec{J}\times\vec{B}$ force which propels the plasma down the barrel.

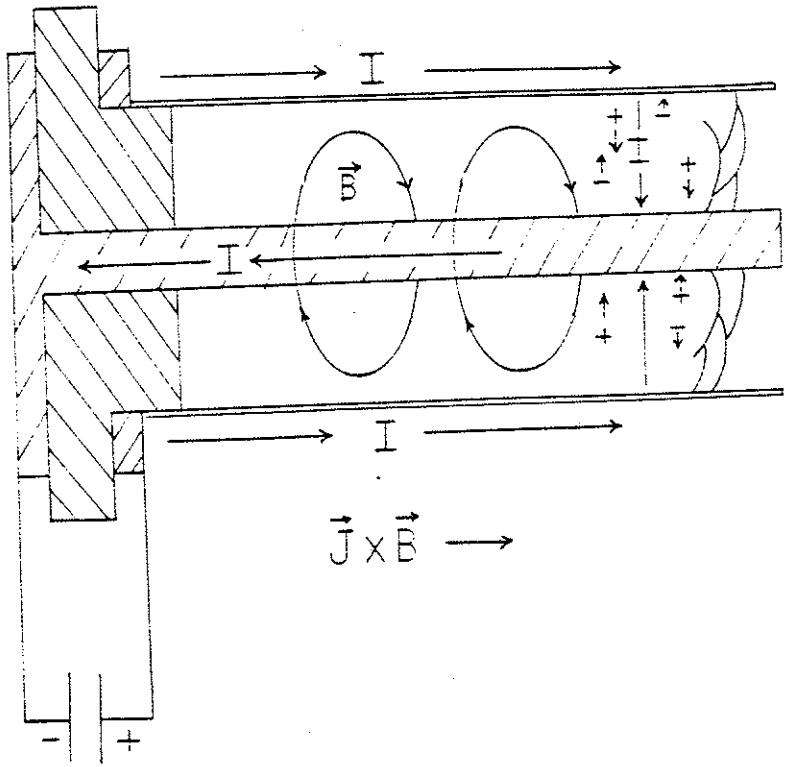

Figure 2-6

gun of this type has a slow component of plasma moving with a directed energy of ~100 eV and a smaller (~%1) component moving near 1 keV. The electrons are moving along with the ions and are usually much colder (<10eV). This is a simple view of what is actually a very complicated process, as evidenced by the lack of homogeneity of the created plasma. This description will be adequate for understanding the experiments that follow, however. A more complete description of the physics of plasma guns can be found in references 4-6 at the end of this chapter.

A schematic drawing of the Marshall gun that was used in these experiments can be found in figure 2-7, with an electrical circuit drawing in figure 2-8. This gun is 55 cm from muzzle to breach with a 5 cm diameter stainless steel outer barrel and a 1.5 cm diameter copper inner barrel. Between the inner and outer barrel there is a 1.25 cm thick Plexiglas insulator which electrically insulates one barrel from the other. This insulator also serves as a vacuum seal.

Gas is puffed into this gun by means of a magnetic valve. This valve is located in the inner barrel 3.5 cm from the breach of the gun. A 60 μF, 5 kV capacitor activates the valve 400 to 600 μsec before the gun is fired. Hydrogen gas is puffed into the gun, and the fill pressure can be varied over a wide range. For most of these experiments the gun was filled to a pressure between 50 mtorr and 200 mtorr. The timing of the gas puff was arrived at by maximizing the amount of plasma trapped by octupole fields upon firing of the gun.

Figure 2-7. Schematic of Marshall gun.

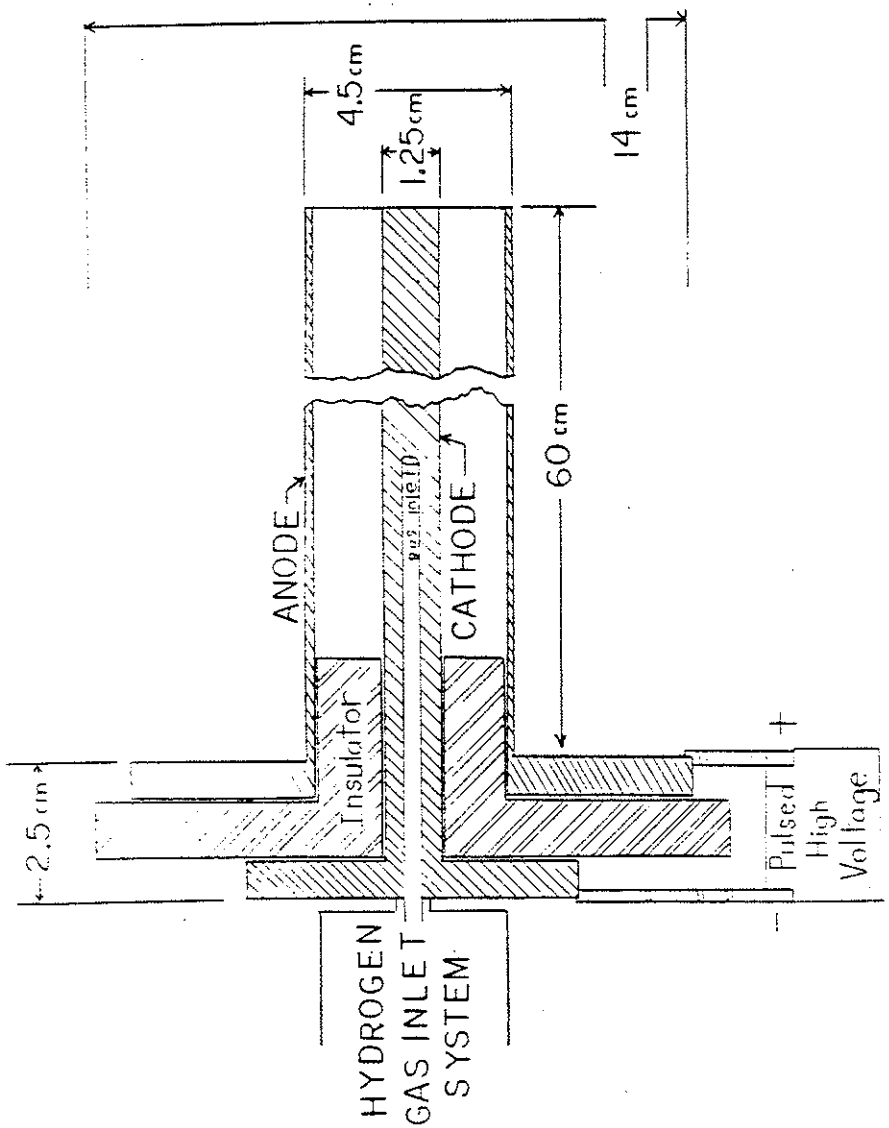

Figure 2-7

Figure 2-8. Electrical circuit diagram for firing Marshall gun.

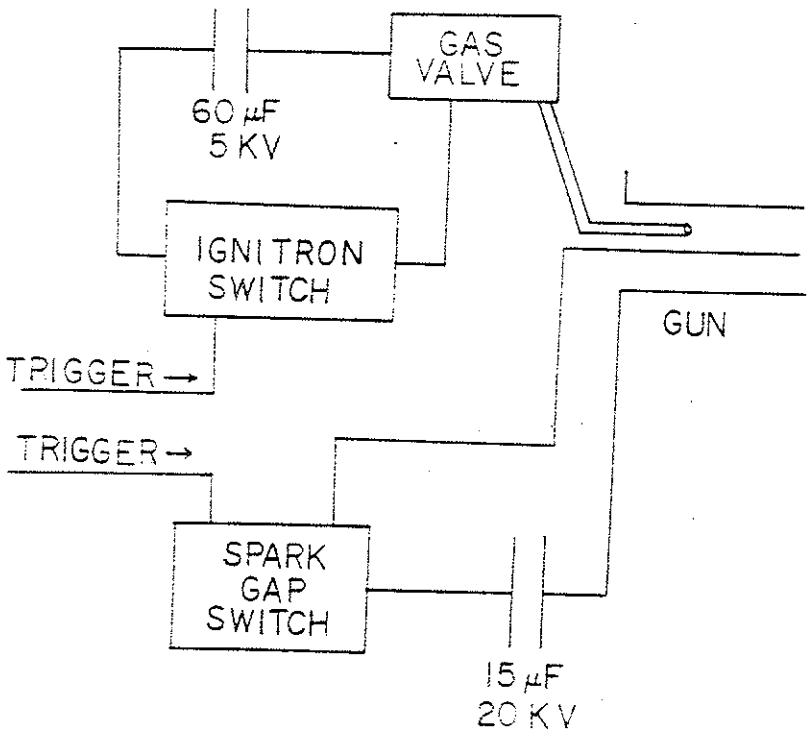

Figure 2-8

The main gun bank consists of a single 15 uF, 20 kV (3 kJ) capacitor. This circuit is triggered by means of a low inductance spark gap which allows the current to rise quickly. This produces a sinusoidal current waveform with a period of about 10 μsec and a maximum current of 200 kA. This current produces the plasma ejected by the gun. A more complete description of the plasma ejected from the gun that was used in this experiment will be given in chapter 2.

C. Interferometer

Plasma density was measured by means of a 70 GHz microwave interferometer (figure 2-9), which has a line of sight down the mid-cylinder of Tokapole II. For the case of a cold, collisionless, unmagnetized plasma the microwave radiation propagates with its wavelength increased from the vacuum value by the factor[7]

$$\mu = \left[1 - \frac{\omega_p^2}{\omega^2}\right]^{1/2}$$

where ω is the microwave frequency and $\omega_p = [ne^2/m\epsilon_o]^{1/2}$, the plasma frequency. If the approximation $\omega^2 >> \omega_p^2$ is used the phase change due to plasma along the path ℓ becomes

$$\Delta\Phi = \frac{e^2}{2m\epsilon_o\lambda_o}\int n_e(\ell)d\ell$$

Figure 2-9. Schematic of interferometer showing reference arm and arm through plasma in Tokapole II which are later mixed for measurement of phase difference.

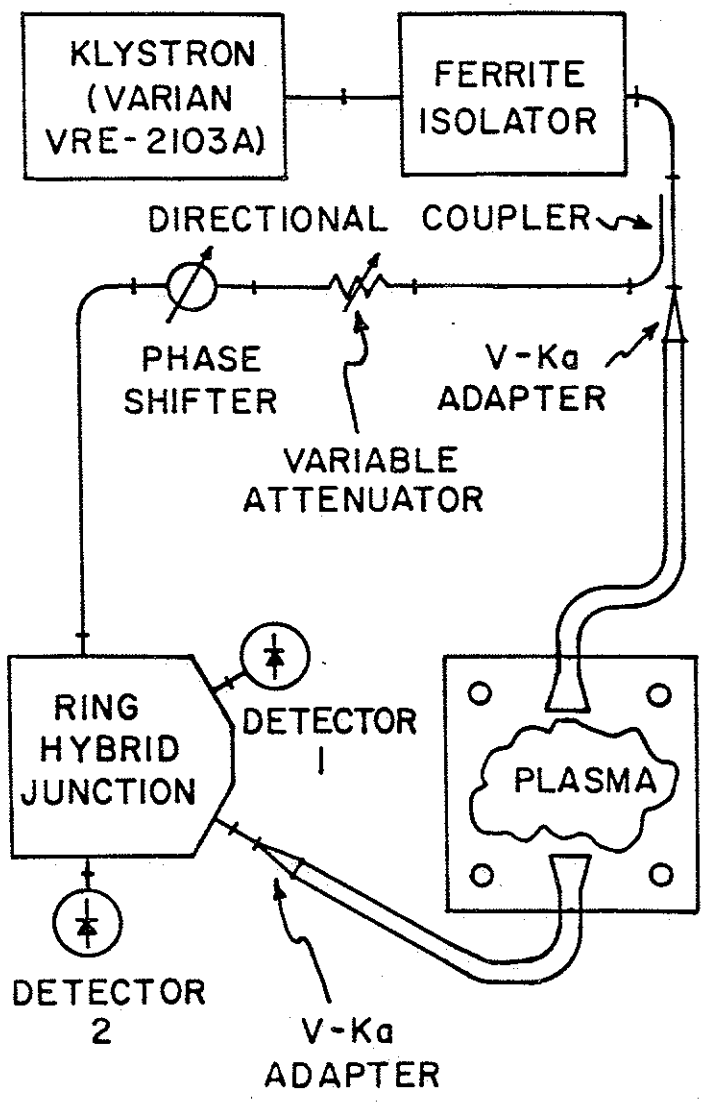

Figure 2-9

where m is the electron mass and λ_o is the wavelength of the microwave radiation in free space. When the density is varied, the phase of the radiation will be seen to change with respect to the reference arm of the microwave system. This measured phase change is then proportional to the line integrated density along the path length, and thus it is a global measurement instead of a local one.

The microwave horns are mounted such that the $\vec{E}$ field of the microwave radiation is parallel to the toroidal magnetic field, since $B_t >> B_p$. This allows the ordinary mode to propagate across the device. The ordinary mode has the same dispersion relation as radiation in an unmagnetized plasma. This makes the equation for phase change as a function of density still valid, even in the presence of a strong toroidal field.

In order to get a density measurement from the phase shift, a Princeton digital interferometer circuit was used[8]. The klystron frequency is modulated by a 1 MHz sawtooth wave. As the klystron frequency varies, a zero-crossing detector senses interference minima due to difference in electrical path length between the plasma arm and the reference arm of the interferometer. The digital circuit, with use of a phase lock loop, detects changes in phase during the 1 usec ramp where the minima occur. A complete 2π phase change of this minimum with respect to the ramp signal represents one microwave wavelength change in optical path length. The digital circuit counts these fringes and then converts the total phase change to an analog density signal.

D. Langmuir Probes

For local measurements of density, Langmuir probes were used. For a complete description of probe theory, see Chen[10], and for a description of the electronic considerations of probe use see Sprott[11].

An ungrounded metal probe inserted into a plasma will reach a steady state floating potential, V_f, such that there is no net current to the probe. If the probe is biased positive or negative with respect to V_f, it will attract or repel electrons, and in the opposite sense ions. This will cause a net current to flow. If the probe is biased negatively enough, all electrons in the area will be repelled and all ions traversing the effective probe area, A (equal to the probe area if the plasma sheath is small), will be collected. This ion saturation current is given by,

$$I_{sat} = \frac{1}{4} n e A v^* \quad \text{where } v^* = \left[\frac{8KT_e}{\pi m_i}\right]^{1/2} \quad \text{for} \quad T_i \ll T_e$$

and where n, m_i, T_i, and T_e are the ion density, ion mass, ion temperature and electron temperature respectively. Thus the density can be determined if the area of the probe tip and the electron temperature are known.

A method of determining the electron temperature,[11] based on measuring the slope of the I-V curve at V_f, was used in conjunction with saturation current measurements to obtain densities. The admittance, Y, is defined as

$$Y = \frac{1}{R} = \frac{dI_i}{dV}\Big|_{Vf} = \frac{eI_{sat}}{kT_e}$$

The admittance can be measured by use of a capacitance bridge that is balanced for zero output signal in the absence of plasma. The addition of plasma unbalances the bridge, and if the output of the bridge is calibrated against known resistances, the admittance, or inverse resistance, of the plasma sheath can be determined. In this way a probe, consisting of two probe tips of the same area, where one is measuring the ion saturation current and the other is measuring the plasma admittance, can monitor the time evolution of the plasma density and temperature at a single point in space.

E. SXR and other Impurity Signals

As a general diagnostic of central plasma conditions of a Tokapole II discharge, soft X-ray radiation, or SXR, signals were used. Radiation in the SXR region in plasmas comes primarily from sources with emissivity strongly dependent on the electron temperature, T_e, so that even though a collimated detector averages

over a chord, the detected signal comes primarily from the hottest point along the chord. The central temperature in a Tokapole II discharge is approximately 100 eV[12]. At this temperature SXR radiation comes primarily from line radiation. Groebner and Dexter determined from doping experiments that radiation from light impurities (carbon, oxygen, etc) accounted for <20% of the SXR signal[13]. At 100 eV the intensity of radiation from metals primarily varies as[14]

$$I \sim n_e n_i e^{-E/Te}$$

where n_e is electron density, n_i is the ion density in the i^{th} charge state, T_e is the electron temperature, and E is the photon energy.

Surface barrier diodes with polypropylene filters were used for SXR detectors on Tokapole II. This detector filter combination allows sensitivity down to a photon energy of about 60 eV. The vertical detector array consists of seven detectors spaced 3.2 cm apart along the outside wall at one toroidal azimuth. Each detector views a spot size of ~3 cm at the midcylinder. The central chord SXR signal was then a good diagnostic for viewing changes in the central current channel's temperature and density.

For general measurement and monitoring of impurity signals, filtered photomultipliers were used. This produced impurity signals for O_{III}, C_{III}, N_{III}, and Cu_I, which are a good monitor of the

cleanliness of the discharge and the impurity concentrations being ejected from the gun into Tokapole II.

F. Data Handling

Most of the data taken for this thesis was handled by a PDP 11/23 computer. Early data however were taken on oscilloscopes and stored on Polaroid film. A LeCroy 8210 digitizer was used in conjunction with the computer. The 8210 is a 4-channel, bipolar, 10-bit digitizer that can digitize up to 10^6 samples/sec. Each 8210 has 32k points of memory that can be divided among the channels used. After each run of data was taken, the data were read on to magnetic tape and transferred to a VAX computer. All of the data analysis was performed on the large computer.

References for Chapter II

[1] A. P. Biddle, R. N. Dexter, R. J. Groebner, D. J. Holly, B. Lipshultz, M. W. Phillips, S. C. Prager, and J. C. Sprott, Nucl. Fusion 19, 1509 (1979)

[2] J. C. Sprott, University of Wisconsin-PLP 744 (1978)

[3] R. J. Groebner, PhD Thesis, University of Wisconsin (1979)

[4] J. Marshall, Phys. Fluids 3, 135 (1960)

[5] L. C. Burkhardt and R. H. Lovberg, Phys. Fluids 5, 341 (1962)

[6] J. Marshall, Proc. High Beta Workshop, Los Alamos, New Mexico, July 28-August 1, 1975, ERDA-76/108, p470

[7] F. F. Chen, Introduction to Plasma Physics, (Plenum Press, New York 1974)

[8] H. R. Garner, University of Wisconsin PLP 833 (1981)

[9] F. F. Chen, "Electric Probes" in Plasma Diagnostic Techniques, R. H. Huddlestone and S. L. Leonard Eds., (Academic Press, New York, 1965), Ch. 4

[10] J. C. Sprott, University of Wisconsin PLP 88 (1966)

[11] J. C. Sprott, Rev. of Sci. Inst. 39, 1569 (1968)

[12]R. J. Groebner, PhD Thesis, University of Wisconsin (1979)

[13]R. J. Groebner and R. N. Dexter, University of Wisconsin-PLP 770 (1978)

[14]G. M. McCracken and P. E. Stott, Nucl. Fusion 19, 889 (1979)

CHAPTER III

GUN INJECTION REFUELING IN TOKAPOLE II

In this chapter the refueling process is characterized with a thorough description of a gun refueled tokamak discharge in Tokapole II. This has relevance to understanding the mechanisms involved in the refueling process itself, but also is important to the fusion community where such characteristics may be very crucial to reactor design. First the injected plasma beam will be described, followed by a short description of a typical tokamak discharge in Tokapole II without gun refueling. A complete description of a gun refueled discharge will then be given, with the important characteristics explained.

A. The Injected Plasma

Measurements of the gun plasma were made using a floating double Langmuir probe. A floating probe was necessary because of the high floating potentials associated with this type of discharge. For these measurements the gun was fired into Tokapole II with no fields present. The Langmuir probe was inserted into the plasma path through a swivel port from above. This allowed placement of the probe at different distances from the gun. A typical trace of the ion saturation current in this situation is shown in figure 3-1.

Figure 3-1. Waveform of ion saturation current from plasma beam streaming by probe.

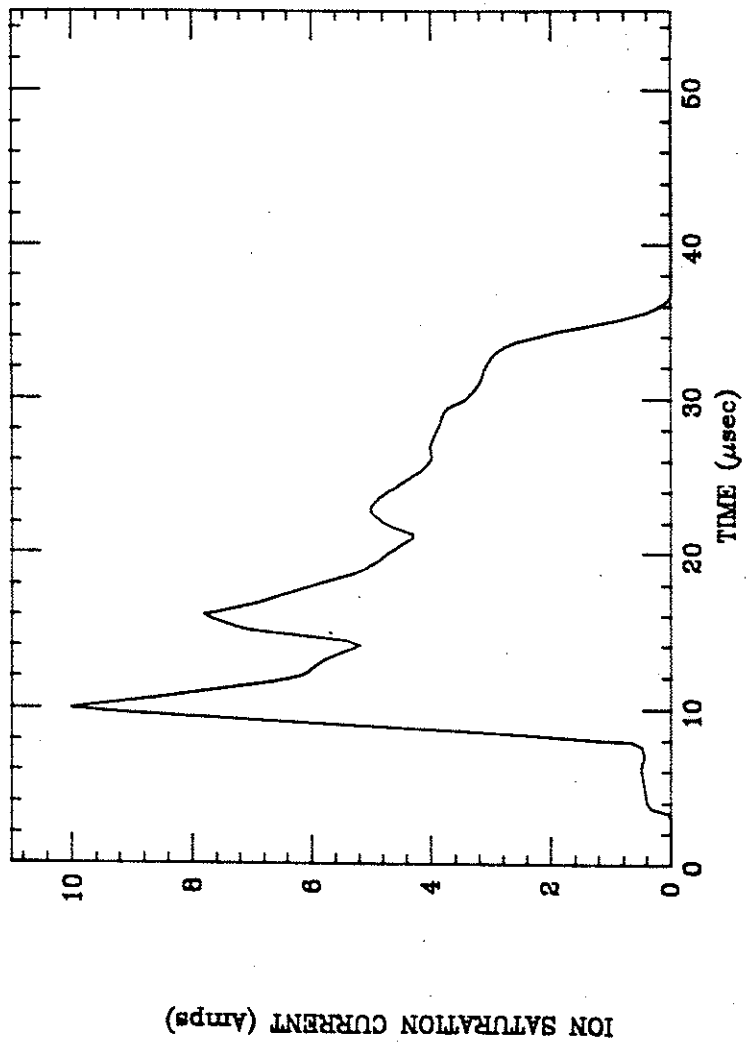

Figure 3-1

The trace was triggered by the rise of current in the gun transmission line. As can be seen, the plasma arrived at the probe several microseconds after current started in the gun. The time of flight of this plasma was measured by placing the probe at different distances from the gun and observing the arrival time of the plasma after the trigger. For gun plasmas used in the refueling experiments, the velocity of the plasma was $\sim 5\times10^6$ cm/sec.

The density of a gun plasma can be derived from the saturation current by using the velocity of the plasma beam. The saturation current is given by

$$j_{sat} = n_b e v_i A$$

where n_b is the beam density, A is the effective probe area, and v_i is the ion directed velocity, which brings new plasma into the probe sheath area. Using this method and the saturation current shown in figure 3-1, the typical gun plasma density was found to be $\sim 1\times10^{15}$ cm^{-3}. There was uncertainty in this measurement because of turbulence, embedded fields and high potentials of the gun plasmas.

In order to confirm this measurement, global measurements of the trapped plasma were also used. First the gun was fired into an octupole field and the average density of the plasma that was trapped was measured by an interferometer. With the known volume of the vacuum chamber at 0.6 m^3 and the dimension of the beam measured by Langmuir probes, a reasonably accurate density can be obtained.

The characteristics of a typical plasma beam that was efficient at refueling are given in the table of figure 3-2. These parameters are not constant however. By changing the voltage on the main gun bank and the gas fill in the gun, the density of the plasma beam and to a lesser extent, its velocity, can be varied over some range. Shown in figure 3-3 is the density trapped by an octupole field as both the gun voltage and gas fill were varied.

A significant amount of neutral gas is also a characteristic of a gun discharge. With a known amount of gas fill, the density trapped in an octupole field implies about a 30% ionization rate, assuming 100% trapping of the plasma. This neutral gas, not ionized by the gun discharge, travels down the gun barrel, at or near the sound speed, after the plasma. The effects of this on the refueling process will be discussed later in this chapter.

B. The Tokamak Plasma

The plasma discharge in Tokapole II is that of a divertor tokamak. Shown in figure 3-4 are the time evolution of several plasma parameters typical of this type of discharge. This is very characteristic of all discharges in which this research was carried out. These three diagnostics were especially important in evaluating the refueling effectiveness.

The first diagnostic is the average density in the discharge as measured by the interferometer. This signal displays the line-averaged density on a chord through the mid-cylinder. Because

Figure 3-2. Characteristics for plasma beam used for refueling.

PLASMA BEAM PARAMETERS

Velocity	5×10^4 m/sec
Pulse Length	20×10^{-6} sec
Length	1.0 meter
Beam Radius	3.0 cm
Total Particles	3.0×10^{18}
Density	1.1×10^{15} cm^{-3}
Electron Temperature	< 5 eV

Figure 3-2

Figure 3-3a. The density trapped in an octupole field as the gun supply voltage is varied.

Figure 3-3b. The density trapped in an octupole field as the gas fill is varied.

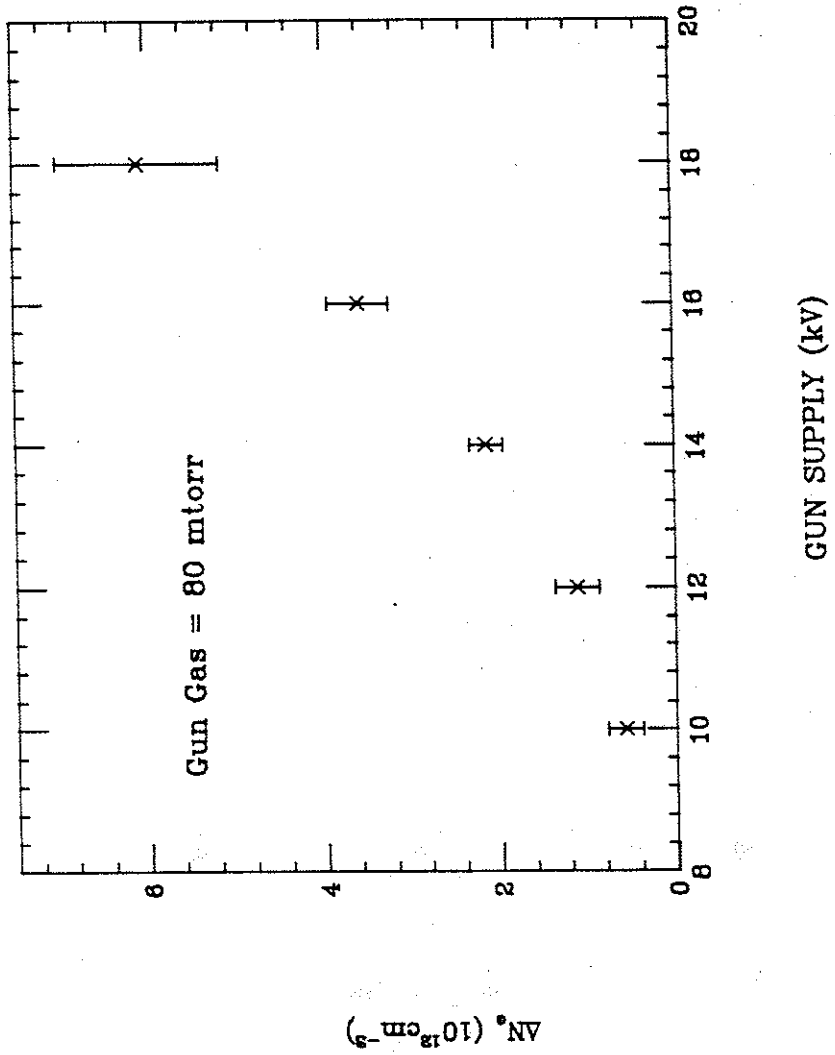

Figure 3-3a

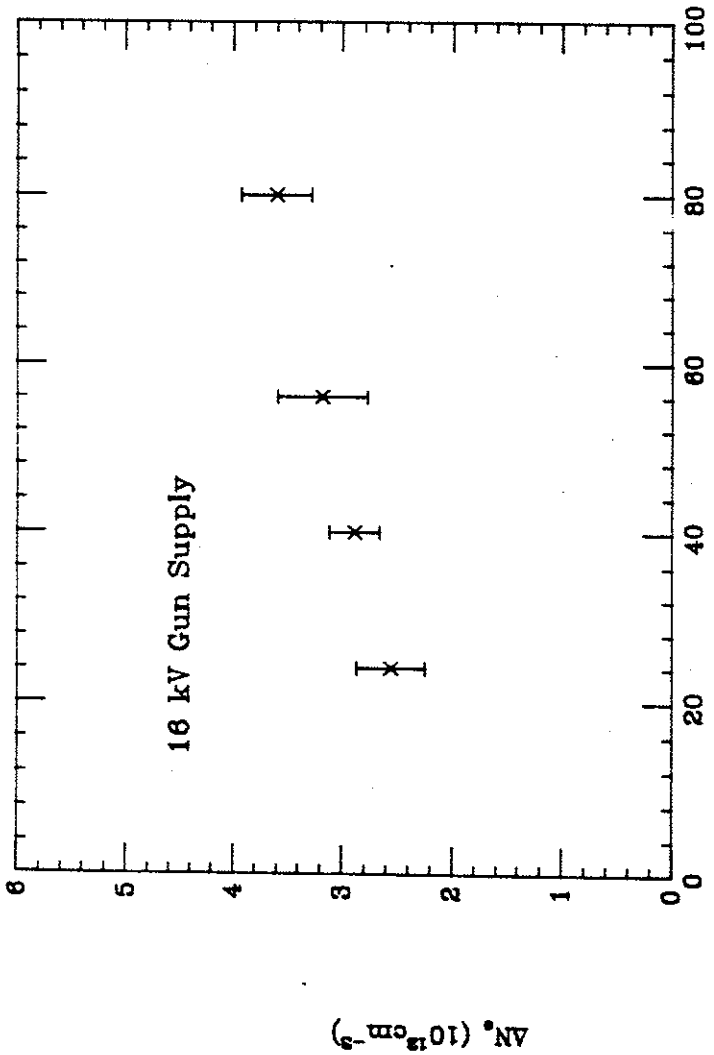

Figure 3-3b

Figure 3-4. Shown are three diagnostic signals for a standard Tokapole II discharge. They are a) line-averaged density from an interferometer, b) central chord SXR signal, and c) plasma current.

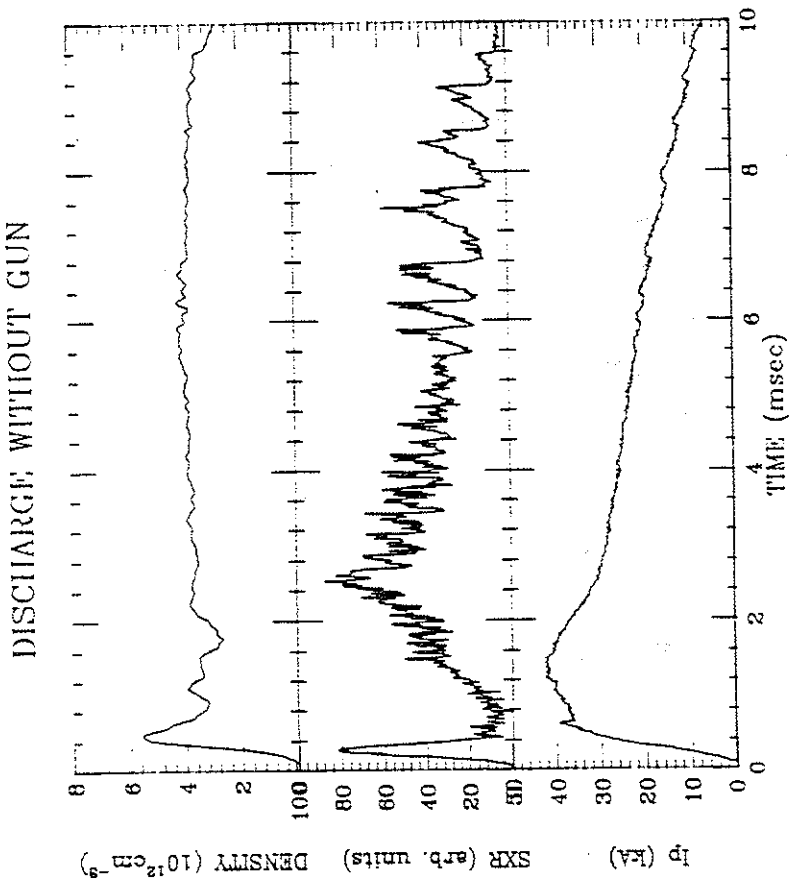

Figure 3-4

the goal of refueling is to add fuel, or density to the discharge, this serves as a basic measure of the effectiveness of the refueling process.

The second diagnostic displayed is the central chord SXR signal. This signal gives a good indication of the relative conditions existing in the central current channel. As explained in chapter 2 the SXR signal depends on both temperature and density. Useful information can be extracted from this diagnostic even though the two parameters are combined together.

The third diagnostic displayed is the plasma current. Plasma current is the mechanism for adding energy as well as providing confinement of the tokamak discharge. This signal characterizes the robustness of the discharge. Also a conductivity temperature of the current channel can be extracted from the plasma current, as will be described next. This also helps to describe the refueling process.

Additional global parameters can be derived if the average density, n_e, the plasma current, I_p, the hoop current, I_h, and the poloidal gap voltage, V_{pg}, are known. This process is documented by Sprott[1] and will be discussed briefly here. Typical values for these parameters are listed in the table in figure 3-5.

If the plasma current is assumed to distribute itself evenly inside the separatrix, then the plasma radius, a, is given by

$$a = 17.4\left|I_p/I_h\right|^{1/4}$$

Figure 3-5. Table of typical derived parameters for a standard Tokapole II discharge.

TOKAPOLE II STANDARD DISCHARGE

Major Radius	50 cm
Minor Radius	10 cm
Toroidal Field	5.2 kG
Hoop Current	200 kA
Plasma Current	25 kA
Average Density	4.0×10^{12} cm^{-3}
Electron Temperature	60 eV
Loop Voltage	4.5 Volts
Safety factor, q	2.2
Energy Confinement Time	0.33×10^{-3} sec

Figure 3-5

This is the radius of a circle with the same cross sectional area as the square-like area inside the separatrix. This area was determined by running computer code calculations with a given I_p and I_h.

After experimental measurements the resistive loop voltage, V_ℓ, seen by the plasma, was fitted to

$$V_\ell = 1/2(1 + t/75)V_{pg} + 0.0045(1 - t/37)I_h - 2.3\dot{I}_p/a^{1/2}$$

where t is time in msec after the start of the discharge and $\dot{I}_p$ is the time rate of change of the plasma current. With this the ohmic input power, P_{oh}, can be calculated from

$$P_{oh} = I_p V_\ell$$

The electron temperature, T_e, can be inferred from I_p, V_ℓ, and plasma radius, a, if we assume Spitzer conductivity with no impurities, $Z_{eff}=1$:

$$T_e = 376(|I_p/V_\ell|/a^2)^{2/3}$$

where the electron temperature, T_e, is measured in eV.

The final parameter to derive is the energy confinement time, τ_E. It is given by

$$\tau_E = \frac{0.144\langle n\rangle_e T_e}{P_{oh}}$$

In this case the entire volume of stable confinement is used and thus this represents a total machine confinement time.

There are numerous approximations in the derivation of these parameters as discussed in reference 1. These parameters, some of which are measured directly while others are inferred, allow observation of gross changes in the plasma behavior due to gun refueling. We can then evaluate the effectiveness of this refueling scheme.

C. The Refueling Process

The effects of gun refueling upon a Tokapole II discharge can be seen in the data of figure 3-6. The most pronounced change in the discharge was an increase in the average density immediately after injection. This is the first requirement for an effective refueling scheme. The interferometer showed this increase to take place in less than 50 μsec after the gun fired. The density rose by ~50% and more or less maintained that to the end of the discharge. If plasma from the gun was deposited into the discharge all at one time, with no other source of fuel, the density should decay after injection with a characteristic particle confinement time. The other source of fuel must be the un-ionized hydrogen gas from the

Figure 3-6. Time evolution of three diagnostics in a gun refueled discharge. They are a) line-averaged density from an interferometer, b) central chord SXR detector and c) plasma current.

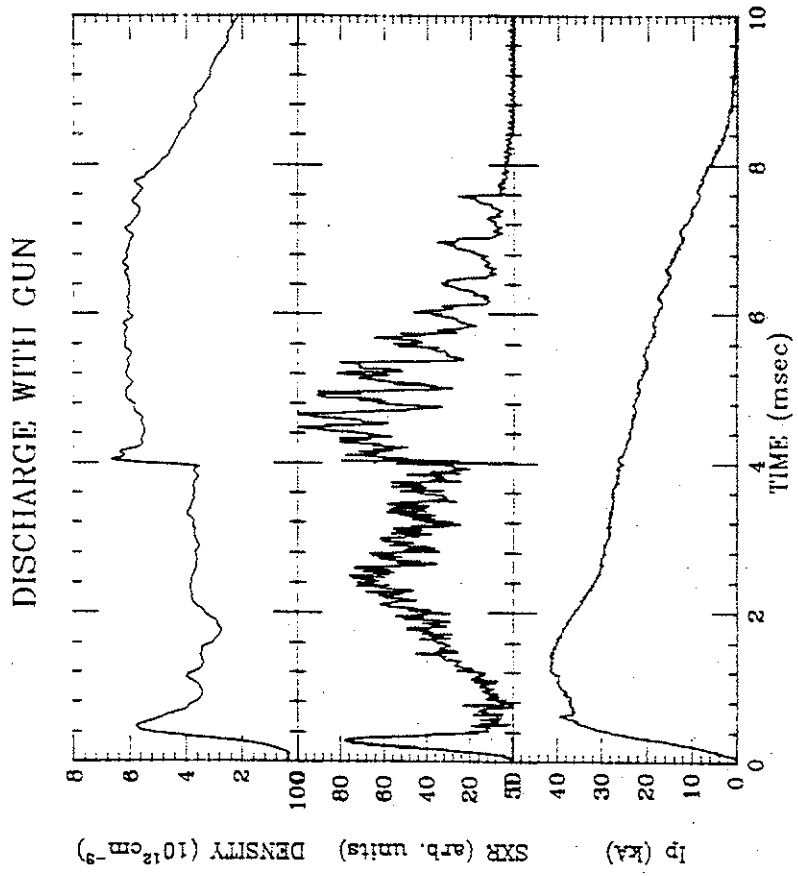

Figure 3-6

gun. As stated earlier only about 30% of the gas that fills the gun is ionized.

If gas from the gun were trapped quickly in the discharge and were responsible for the rapid rise in density, then the gun would be no better than an efficient gas puffer. If this were true the gun would not scale up well to larger tokamaks. In order to determine if the rise in density was just a gas fueling effect, the gun was filled with gas but not fired. Shown in figure 3-7 is the density for two different discharges. The first is a standard gun refueled case, and the second is the case of filling the gun with gas and not firing it. For the gas case the average density did not start to rise until 2-3 msec after the gun would have fired. Apparently the gun firing was responsible for the rapid increase in density. To better illustrate this, the signal from case II was subtracted from case I and is shown in figure 3-8. This signal should contain the effect of just the gun discharge and not the gas that later leaves the gun. As can be seen the density due to the gun discharge rises immediately and then decays with a time consistent with the expected particle confinement time. The fact that this signal goes negative late in time is due to the gun refueled discharge having ended slightly before the gas refueled case. This problem of late gas could be cured on this or other gun refueling systems by several techniques such as a fast shutter.[2]

Figure 3-7. Line-averaged density for two discharges. They are a) a gun refueled discharge, and for b) gun filled with gas but not fired.

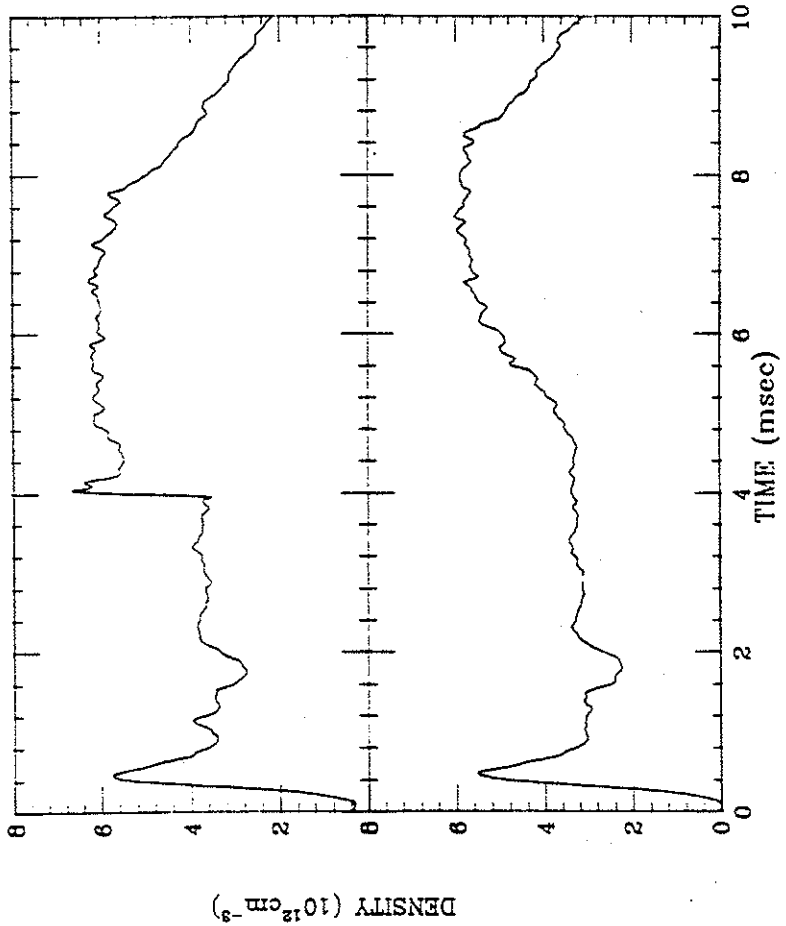

Figure 3-7

Figure 3-8. Line-averaged density from an interferometer for a discharge with gun filled with gas but not fired, subtracted from a gun refueled discharge.

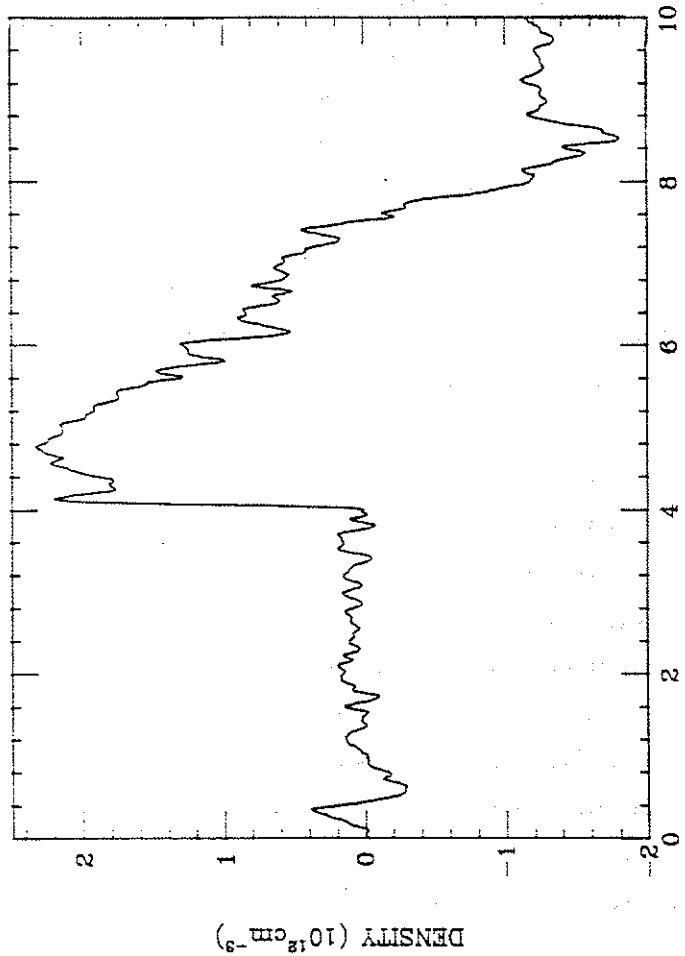

Figure 3-8

The rapid rise in density might also have been caused by energetic neutrals. Neutral hydrogen atoms that were energized by the gun discharge could have traveled at very nearly the speed of the plasma beam and then been ionized by the plasma discharge. In chapter VI it will be shown that the trapping mechanism is not a collisional process. The neutrals need collisions to become plasma and thus are not responsible for this density rise.

The central chord SXR signal also shows changes due to the gun. This signal which is proportional to density in the center and exponentially dependent on temperature does not rise immediately. But 1/2 to 1 msec after the gun fired, the signal rose to a value 2 to 3 times what it would have been without gun refueling. Apparently the gun deposited significant amounts of cold plasma in the center of the discharge. The plasma current then ohmically heated this plasma until an equilibrium was reached. This should have taken an energy confinement time, which was approximately 0.33 msec. The added cold plasma required more input power to heat it up. This additional input power is evidenced by the small decrease in the plasma current for the gun refueled case. The increase in input power, P_{oh}, was supplied by the $-L\frac{dI_p}{dt}$ term in the expression for the resistive loop voltage, V_ℓ. This decrease in I_p means that the equilibrium temperature was slightly lower. The increase in the SXR signal signifies that the central density must be increasing if there is no increase in temperature. Another possibility is an increase in impurities responsible for radiation

in the SXR region. Later in this chapter that will be shown not to be the case.

For efficient refueling it is desirable to deposit as much of the plasma as possible in the center of the discharge. In order to determine where gun refueling was depositing plasma, profiles before and after injection were taken with two different diagnostics. The first profile was taken using the SXR vertical array that exists on the outer wall. These detectors which are separated by 3.2 cm look perpendicularly inward towards the mid-cylinder. The signal from each detector is associated with the hottest part of the discharge along its line of sight. In this way the array represents a radial profile of the SXR emissivity. Figure 3-9 shows a radial profile of the SXR emissivity with and without injection.

It can be seen in figures 3-4 and 3-6 that the central chord SXR signal is modulated very strongly by sawtooth oscillations. To avoid error caused by measuring the SXR signal at different phases of a sawtooth oscillation for discharges with and without gun injection, each point of the profile was taken very near the peak of a sawtooth oscillation just after the gun injection.

The data shows clearly that gun injection has caused the profile to become more peaked. This profile does not necessarily represent the density, but whatever gun injection is doing to the discharge it is affecting the center most strongly.

Figure 3-9. Chordal profile of SXR emissivity with and without gun injection.

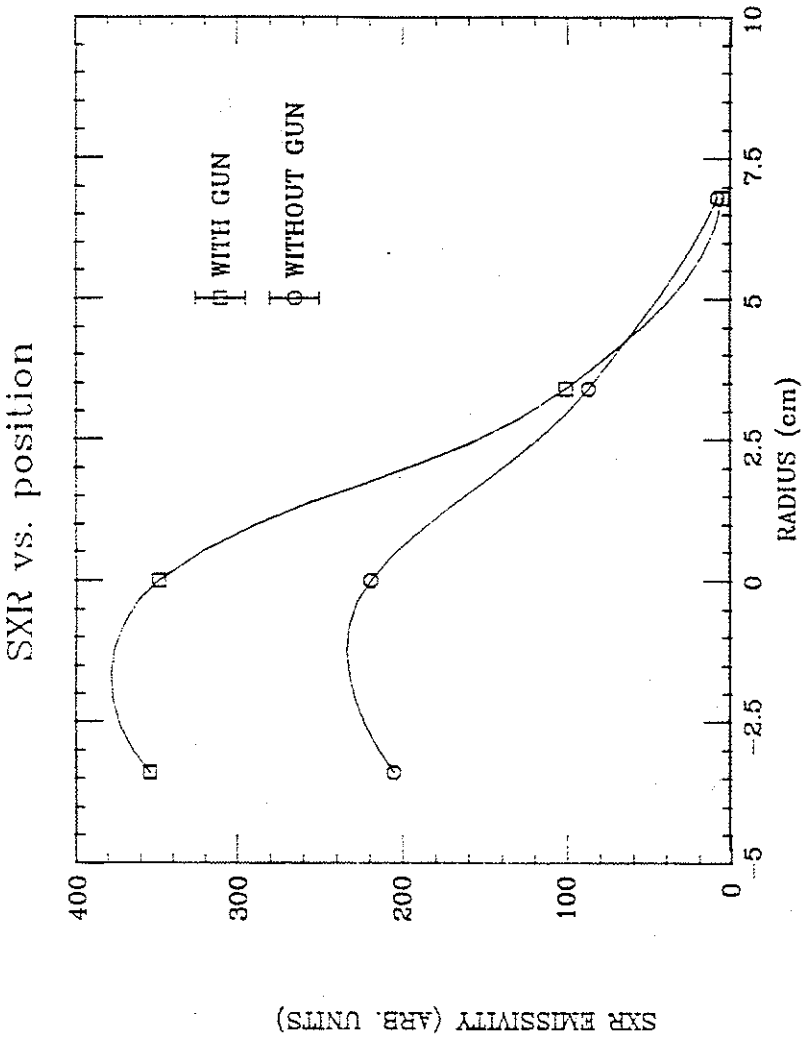

Figure 3-9

To better understand how the density profile was affected by gun-injection, Langmuir probes were used in conjunction with the interferometer. Langmuir probes could be inserted into the edge of the discharge up to the separatrix, or the edge of the current channel, before they were destroyed by the plasma current. This was about 12 cm from the wall, or 10 cm from the center of the discharge. A probe stalk which contained a Langmuir probe and an admittance probe was used over this range to get an edge density profile. This edge profile was taken for a gun-refueled case at a time of ~150 μsec after injection and for a nonrefueled case at the same time during the discharge. Each of these cases also has associated with it a line-integrated density value obtained from the interferometer. With these two different diagnostics, information about the density in the center of the discharge can be inferred.

To obtain a profile using probes and the interferometer, the edge density profile was line-integrated, and then subtracted from the interferometer signal. The remaining value represented a line-integrated density over the central plasma, inside a radius of 10 cm. This signal was then smoothed into a central density profile as a continuation of the edge density profile. This was done making sure the final density profile had a line-integrated value that corresponded to the interferometer value. The result of this process is the inferred density profiles of figure 3-10. This figure contains profiles of the refueled and non-refueled case. The gun refueled discharge had a much higher value for the central

Figure 3-10. Density profile inferred from interferometer in conjunction with edge Langmuir probes for discharge with and without gun refueling.

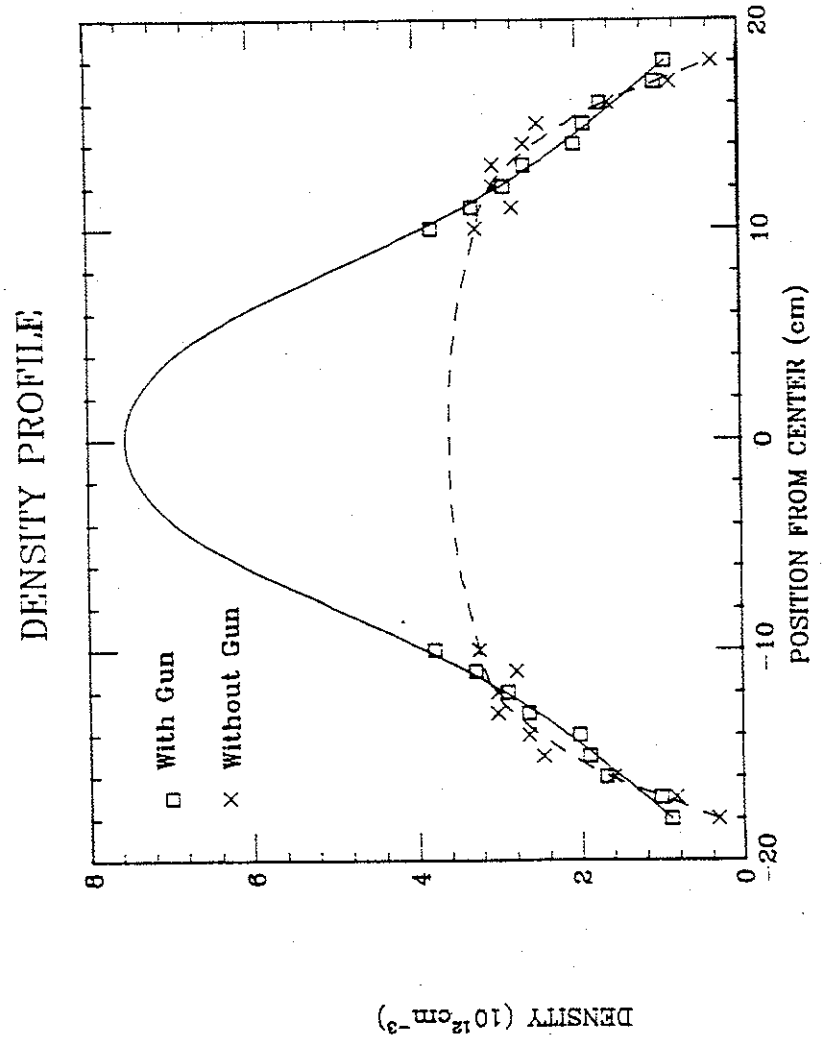

Figure 3-10

density, while the edge densities for the two cases were very similar. The gun was depositing most of its plasma in the center of the discharge.

There were a few assumptions and approximations made in inferring this density profile. First, there was some liberty in choosing the exact shape of the density profile over the center. There was also uncertainty in the absolute magnitude of the probe data, due to such factors as magnetic field and sheath size[2]. This could possibly have led to the non-refueled case having a more peaked central profile than is shown. If this were the case, then the gun-refueled case would also have been affected the same way. The important point is that the line-averaged density was increased 30% to 50% by gun-injection with little or no discernible change in the edge density. All of the plasma was deposited in the center of the discharge.

D. Energy Confinement

Energy confinement in tokamaks has been fit, in the past, to the Alcator scaling law[3]. This empirical scaling law states that the energy confinement time, τ_E, is proportional to the plasma density. At the highest densities in tokamaks, τ_E is seen to fall below this equation[3]. Pellet refueling has restored Alcator scaling at the highest densities, presumably due to peaking of the density profile[5].

On Tokapole II the confinement time was measured to see if gun refueling would increase the energy confinement above that observed with gas puffing. The results proved to be inconclusive. By measuring the energy confinement time as described earlier in this chapter, the table in figure 3-11 was obtained.

Three cases were examined. The first was a standard non-refueled tokamak discharge as shown in figure 3-4, and the second was the gun-refueled case of figure 3-6. The final case was obtained by additional gas puffing to raise the density to that of the gun-refueled case. The confinement time was calculated at intervals of 0.5 msec after the gun fired.

The confinement time τ_E is increased slightly in the gun-refueled case above the standard discharge and extra gas case. The changes in τ_E were small, however, and may fit within the uncertainty of the measurement. Gun-refueling was apparently not a better scheme for refueling than gas puffing on Tokapole II, from an energy confinement point of view. This was probably due to the small size and low densities of Tokapole II. Gun-refueling is more important for large tokamaks where gas puffing may be inefficient. When gun-refueling is carried out on large tokamaks the results of pellet injection might be reproduced.

Figure 3-11. The energy confinement time, τ_s, in 0.5 msec intervals for three separate cases. They are for a) a standard discharge, b) a gun refueled discharge, and c) a standard discharge with extra gas puffing.

ENERGY CONFINEMENT FOR 3 CASES

	τ_E (msec)		
Time (msec)	Std. discharge	Gun Refueling	Extra Gas
0.5	.00	.00	.00
1.0	.04	.04	.03
1.5	.03	.03	.03
2.0	.03	.03	.03
2.5	.08	.08	.07
3.0	.19	.19	.19
3.5	.23	.22	.24
4.0 (Gun Fires)	.29	.20	.24
4.5	.28	.29	.28
5.0	.28	.35	.30
5.5	.34	.51	.29
6.0	.37	.28	.31
6.5	.34	.31	.34
7.0	.29	.25	.19

Figure 3-11

E. Impurity Generation

An issue of concern for tokamaks is impurity contamination. Heavy impurities will radiate energy and cool the plasma. It is desirable to keep them to a minimum. Gun injection has the potential to generate many impurities, especially from sputtering of the electrodes during the arc discharge. On Tokapole II several impurity signals were routinely monitored to observe machine cleanliness. These impurity lines are C_{III}, O_{III}, N_{III}, and Cu_I.

The impurity signals for a gun refueled discharge are shown in figures 3-12 and 3-13. Early in time during start-up the signal is large. This is due to the strong interaction of the plasma and the machine wall before a stable equilibrium is established[6]. After start up the impurity radiation level receded to some equilibrium level. When the gun fired, there was a small increase in the impurity levels that quickly died away. Gun refueling did not increase impurity radiation significantly.

Optimizing the gun to produce fewer impurities was not one of the goals of this work. Yet, the impurity production remained at an acceptably low level. This is encouraging for the possibility of using gun-refueling for a reactor. With some work it seems likely that a Marshall gun could be clean enough for use in a reactor.

Figure 3-12. Impurity radiation for N_{III} and O_{III}. Gun fires at 4.5 msec.

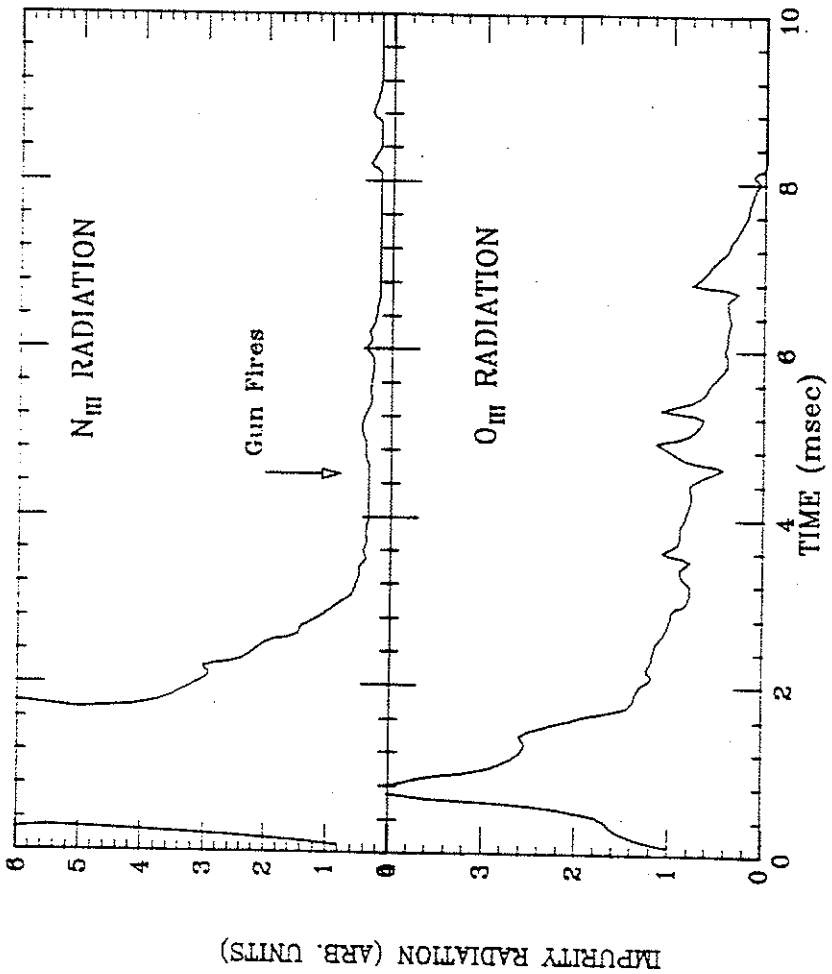

Figure 3-12

Figure 3-13. Impurity radiation for C_{III} and Cu_I. Gun fires at 4.5 msec.

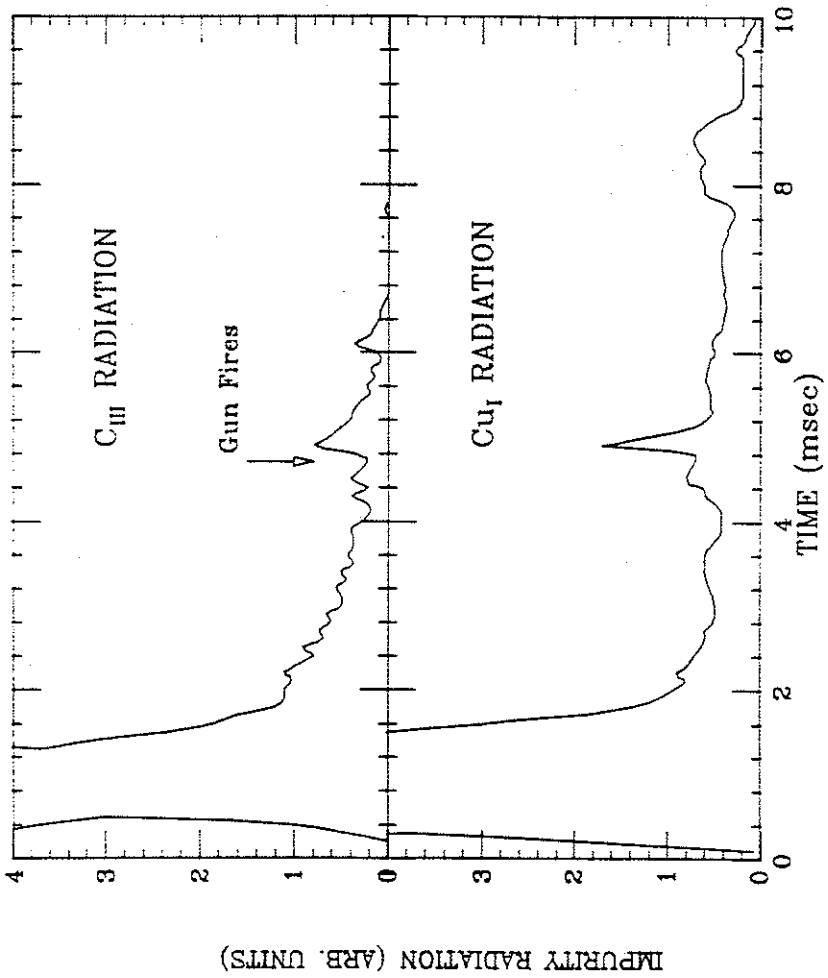

Figure 3-13

References for Chapter III

[1] J. C. Sprott, University of Wisconsin-PLP 889

[2] G. Kuswa, Rev. of Sci. Instr. 37, 189 (1966)

[3] F. F. Chen, "Electric Probes" in Plasma Diagnostic Techniques, R. H. Huddlestone and S. L. Leonard Eds., (Academic Press, New York, 1965), Ch. 4

[4] M. Murakami, Phys. Rev. Lett. 42, 655 (1979)

[5] S. Fairfax et al., Proceedings of the Eighth International Conference on Plasma Physics and Controlled Nuclear Fusion Research, (International Atomic Energy Agency, Brussels, 1980), Vol. 1, p. 439

[6] M. Greenwald, D. Gwinn, S. Milora, J. Parker, R. Parker, S. Wolfe, et al., Phys. Rev Lett. 53, 352 (1984)

[7] N. S. Brickhouse, University of Wisconsin PhD Thesis (1984)

CHAPTER IV

A MODEL FOR THE TRAPPING OF GUN-INJECTED PLASMA

A. Introduction

A moving beam of plasma has the ability to cross magnetic field lines by setting up a polarization electric field[1]. As the beam encounters the magnetic field, electrons are deflected in one direction and ions the other. This continues until an electric field builds up to allow the interior of the plasma beam to $\vec{E}\times\vec{B}$ drift its way across field lines. This moving plasma can be stopped if an external conductor shorts out the polarization field. As the moving plasma tries to reestablish the polarization field, the resulting current will create a $\vec{J}\times\vec{B}$ force to slow the plasma down. Baker and Hammel[2] showed that this model could accurately represent a physical experiment.

Experiments, in which a gun plasma was injected into an octupole field, extended this model to different magnetic configurations with interesting results[3]. The toroidal octupole has only poloidal field, with none in the toroidal direction. In this case the magnetic field lines provide the mechanism for shorting out the polarization field.

In figure 4-1 a plasma beam is shown encountering a purely circular poloidal field, which is an idealization of the octupole field. As the beam encounters the magnetic field a polarization field is set up to allow the plasma to keep moving. As the plasma crosses to the center and then to the other side of the device, the magnetic field lines change direction with respect to the moving plasma. The polarization field must also change in response to this. This shifting will cause an electric field in the direction of travel to be set up along the outer edges of the plasma beam.

The electric field in the direction of $\vec{v}$ causes a current to flow perpendicular to $\vec{B}$ and in the direction of travel. This current is shown as $\vec{J}_D$ in the figure. The conductivity across field lines is smaller than along field lines, but enough current can flow to deplete the polarization charge and field. The plasma beam then attempts to reestablish the polarization field with a polarization current, $\vec{J}_P$. A current loop is thus set up in the plasma with polarization and depolarization currents, $\vec{J}_P$ and $\vec{J}_D$ respectively. This current loop will slow down the plasma. Both legs of $\vec{J}_P$ produce a $\vec{J}_P\times\vec{B}$ force in the $-\vec{v}$ direction while the $\vec{J}_D$ leg of the current loop produces no net force on the plasma.

These polarization and depolarization currents were measured for a plasma injected into a toroidal octupole.[3] The observed currents were large enough to stop the plasma in the device. The result of the experiment was consistent with this model.

Figure 4-1. The mechanism for trapping a plasma beam in poloidal fields. Reversal of the magnetic field allows depolarization current, J_p to flow. The resultant current to support it, J_p, produces a $\vec{J} \times \vec{B}$ force to slow the plasma.

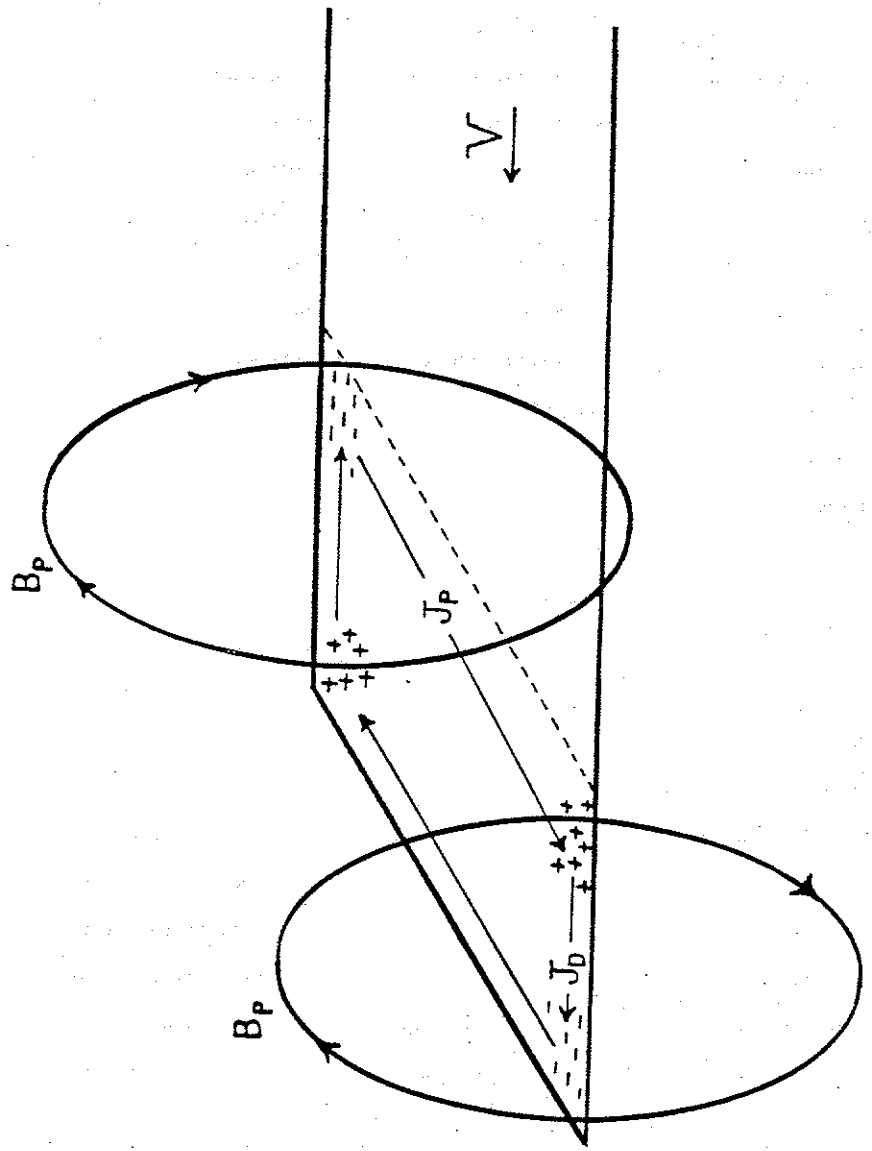

Figure 4-1

A complete and thorough description of this process can now be illustrated, but first a few comments about the current paths are necessary. There are two possible paths the current $\vec{J}_D$ could travel in figure 4-1. Besides the path shown, the current could also flow along field lines, instead of across them, to reach the other side of the device. This current path would also short out the polarization field. A quick calculation shows that conductivity along field lines, for a typical magnetic field strength, should be, at a minimum, an order of magnitude greater than across field lines. Measurements showed that the current flowed parallel to the direction of travel, $\vec{v}$, perpendicular to field lines.[3] Current flow along field lines was not observed and thus will not be considered. In fact, this current parallel to $\vec{B}$, would be ineffective if a weak toroidal field, 1/10 the strength of the poloidal field, were added. This would cause the poloidal field lines to not line up, and an effective depolarization current would not flow. In reality such an added toroidal field barely affects trapping.

Another possible current path to short out the polarization field is perpendicular to both $\vec{B}$ and $\vec{v}$. This current would flow parallel to a cross section, but along the outer edge of the beam. The $\vec{J}\times\vec{B}$ force of this current flow, however, would just cancel the force of the polarization current that supports it. Thus we will consider only a depolarization current strictly parallel to $\vec{v}$, across the magnetic field.

B. The Trapping of Plasma in a Poloidal Field

An idealized case of plasma being injected into an octupole field will now be considered. This case is less complicated than the more general one of injection into a combination of poloidal and toroidal fields, as is the case for a tokamak. This will serve as an exercise to illustrate the procedure for the more general case to follow.

For a plasma beam traveling along the midplane and perpendicular to the magnetic axis, the magnetic field through the center of the device can be approximated by a function proportional to r^3 as shown in figure 4-2. Refer to figure 2-4 for a diagram of the field that this represents. The origin is in the center of the device and the distance L/2 can be any distance of interest from the center of the machine. The functional form of the magnetic field strength with this approximation is given by

$$|B| = -B_o\left\{\frac{2x}{L}\right\}^3 \qquad (4\text{-}1)$$

The injected plasma beam is modeled as a rigid column of square cross section as shown in figure 4-3. The plasma is modeled as a rigid column to simplify the equations that follow into a solvable form. This approximation should not change the underlying physics of the problem. The plasma column has width 2a on each side, with

Figure 4-2. Idealized poloidal field as a function of x.

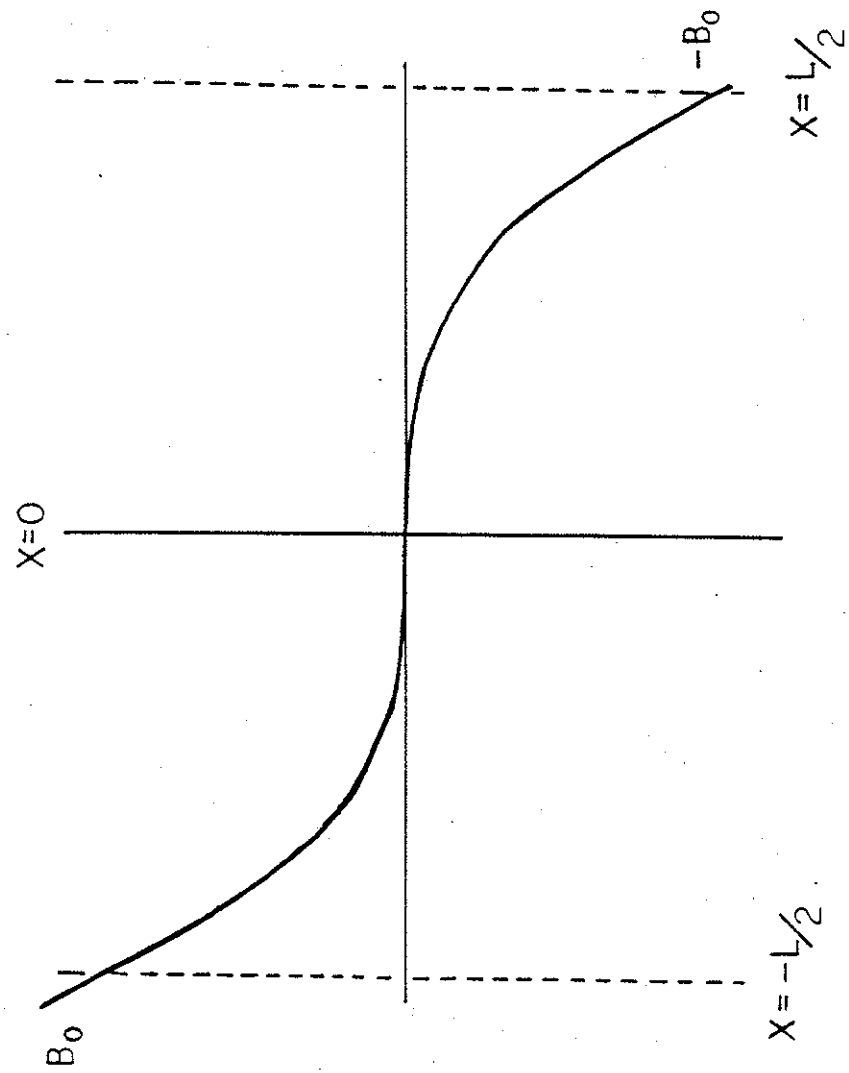

Figure 4-2

Figure 4-3. The injected plasma is modeled as a rigid column crossing the magnetic field structure

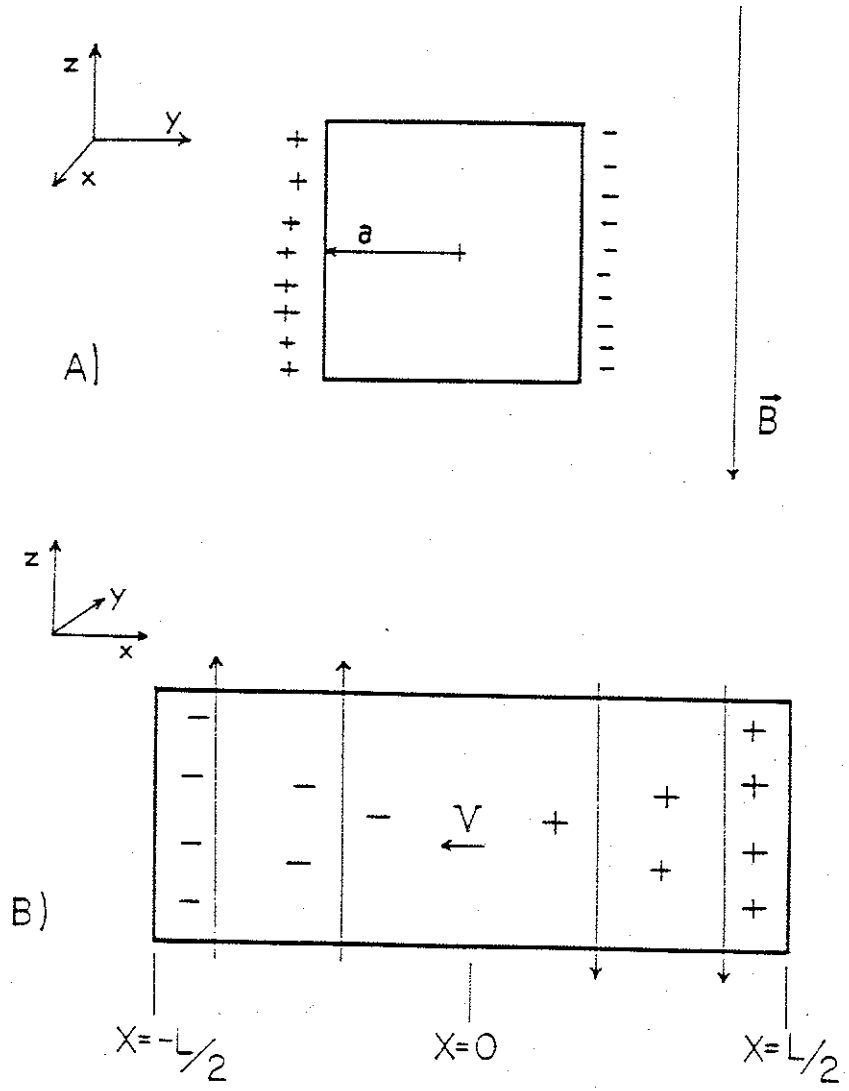

Figure 4-3

length L in the direction of motion. The direction of magnetic field is also shown in the figure to help with orientation.

With the given conditions for plasma to cross a magnetic field, the interior of the plasma sees an electric field,

$$\vec{E} = -\vec{v} \times \vec{B} \tag{4-2}$$

The outer edges of the column with sides parallel to $\vec{B}$ would then be at a potential given by,

$$\phi(x) = B(x)va \tag{4-3}$$

where $\phi(0)$ is taken to be zero. Because $|B|$ varies as a function of x, ϕ does also. This creates an electric field, $\frac{d\phi}{dx}$, in the x direction, which in turn causes a depolarization current, $\vec{J}_D$, to flow. The current density flowing along the edge of the plasma is given by

$$J_x = \sigma \frac{d\phi(x)}{dx} \tag{4-4}$$

where σ is the conductivity of the plasma along the outer edge of the plasma column subject to this electric field. The total current flowing on one side is then

$$I(x) = A\sigma \frac{d\phi(x)}{dx} \tag{4-5}$$

where A is the effective conducting area along the outer edge of the column. The conducting medium is the plasma along the edge of the column that has been stopped by the magnetic field and does not see all of the polarization electric field.

The current in the x direction is the depolarization current that depletes the polarization charge. The plasma column will then support a current through it to maintain the polarization field. The current density through the column would then be given by

$$J(x) = \frac{1}{2a} \frac{dI(x)}{dx} \tag{4-6}$$

as shown in figure 4-4. This results in a current density inside the plasma column of

$$J(x) = \frac{A\sigma v}{2} \frac{d^2B}{dx^2} \tag{4-7}$$

A slowing force is acting on the plasma column due to this current flowing perpendicular to $\vec{B}$ through it. An element in the plasma sees a force

$$mn_b \frac{d\vec{v}}{dt} = \vec{J} \times \vec{B} \tag{4-8}$$

Figure 4-4. Polarization current flowing through the plasma column.

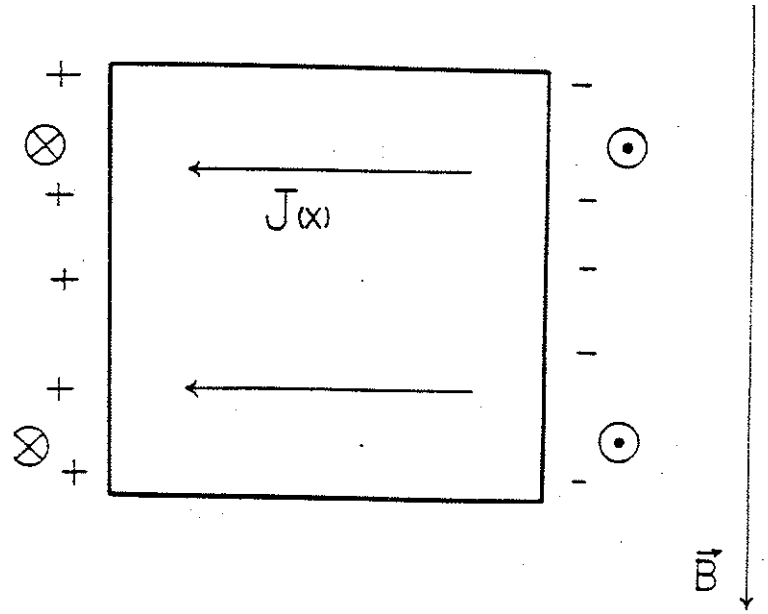

Figure 4-4